ACTIVE STABILIZATION OF A CAR-TRAILER SYSTEM BY MEANS OF TORQUE VECTORING

Michele Vignati*, Sidharth Dave and Federico Cheli

Politecnico di Milano,
Department of Mechanical Engineering,
via La Masa 1, 20156, Milano MI, Italy
Fax: +39 02 2399 8492
Email: michele.vignati@polimi.it
Email: sidharth.dave@mail.polimi.it
Email: federico.cheli@polimi.it
*Corresponding author

Absract: The addition of a trailer to a vehicle introduces significant changes to its dynamic behaviour. Therefore, the response of the vehicle to driver inputs and external excitation differ and are in turn functions of the parameters of the system. The lateral response of the system is of significant interest as unfavourable conditions may lead to instability in the system. The instability introduced may cause the vehicle to stray from the intended path, and in extreme situations may even cause the vehicle to topple over. This instability may be introduced by means of manoeuvres performed by the driver, like a lane change, or may even be triggered by external factors such as lateral forces arising because of wind. This phenomenon has been studied in-depth, and numerous active systems have been proposed. However, the systems in use exploit brake distribution in the wheels of the vehicle. Electric vehicles with independent motors provide the opportunity of achieving the same through torque vectoring. This paper proposes a feedback-loop control system as an active driver assistance system that enables stabilisation of the system by means of torque vectoring for an independent motor two-wheel drive electric vehicle.

Keywords: Vehicle Dynamics; Control System; Vehicle-Trailer System; Torque Vectoring

Biographical notes: Michele Vignati received his master degree (2013) and PhD (2017) in mechanical engineering in Mechanical Department of Politecnico di Milano with thesis on control strategies for distributed powertrain of hybrid and electric vehicles. From 2019 he is Assistant Professor (RTDA) in the research field of applied mechanics. In particular, he focuses on mechanical systems dynamics and control applied in the automotive field. He worked on tire dynamics and modelling in cooperation with Pirelli while in the last years he is also working in autonomous driving field.

Sidharth Dave Sidharth Dave received his bachelor degree in Mechanical Engineering from Manipal Institute of Technology in 2014. He worked with Tata Motors Ltd. for 1 year as a Service Engineer in 2015. In 2020 he received his Master of Science in Mechanical Engineering with a focus in ground vehicle

engineering from Politecnico di Milano.

Federico Cheli graduated in Mechanical Engineering in 1981 at the Milan Polytechnic. In 1983 he was appointed university researcher, in 1992 a second-level university professor and since 2000 he is full professor at the Faculty of Industrial Engineering of Politecnico di Milano. The scientific activity mainly concerned research on dynamic behavior of vehicles, road and rail, as weel as large structures subjected to wind and traffic; identification of the parameters of mechanical systems and their control; modeling and testing of the tire and its interaction with the vehicle; studies on the aerodynamics of rail and road vehicles; studies and design of hybrid / electric vehicles. He is currently chairman of the board of the mechanical engineering course of the faculty of industrial engineering of the Politecnico di Milano; he is a member of the University Didactic Coordination Body. He is part of the Board of the Applied Mechanics Group and of the kinematics and dynamics group of the multibody systems of the Italian Association of Theoretical and Applied Mechanics. He is coordinator of numerous national research projects (PRIN) and Europe and responsible for a series of research contracts between the Politecnico di Milano and national and international companies. Member of the editorial board of the International Journal of Vehicle Performance and of the International Journal of Vehicle Systems Modeling and Testing.

1. INTRODUCTION

The addition of a trailer to a vehicle significantly alters its dynamic behaviour. In a study by Weiven Deng and Xiaodi Kang (Deng and Kang, 2003), it was shown that the effective damping of the vehicle-trailer system is considerably lower as compared to the vehicle alone case, resulting in an excessively oscillatory response in both hitch angle and hitch angle rate, especially under low-friction conditions and high speeds. Further, the vehicle exhibits a slower response when coupled with the trailer. Various studies ((Deng and Kang, 2003), (Hac, et al., 2008)) have shown that two types of instabilities are generally observed in articulated vehicles or vehicles with trailers/semi-trailers.

The first type of instability is divergent in nature. It occurs above a certain critical velocity, and the hitch angle increases without experiencing oscillations. This condition leads to jack knifing.

The other type of instability is dynamic in nature. This instability leads to generation of an oscillatory motion of increasing amplitude in the trailer, known as snaking or trailer sway. In particular, in the study by Mohamed Bouteldja and Veronique Cerez (Bouteldja and Cerezo, 2011), it was shown that jacknifing occurs when the angle between the tractor and the semi-trailer becomes superior to 90 degrees. The driving wheels of the tractor lose their skid resistance and are involved towards the right-hand side or the left because of the force exerted by the trailer. In a study by J. Darling and others (Darling, et al., 2009), it was shown that divergent oscillation is often associated with high speed and an initial impulse caused by a driver's steering input, wind gusts, uneven roads, or the passing of large vehicles. Instability may also be induced while overtaking or being overtaken by large trucks at excessive speeds (Darling and Standen, 2003).

Trailer oscillations are induced beyond a certain critical velocity, which in turn, is dependent on the parameters of the towing vehicle and the trailer. Some of these parameters are design based, such as trailer and vehicle wheelbase and cornering stiffness of the tyres. While some are based on the operating parameters, such as yaw inertia of the trailer, position of the centre of mass of the trailer and ratio of mass of the vehicle and the trailer. To minimise the negative impact of a trailer on the vehicle, the desired configurations are those which have a large vehicle-trailer mass ratio, low trailer yaw moment of inertia and a long trailer tongue length (Deng and Kang, 2003).

Since vehicles and trailers are conceived separately, and the onset of instability depends not just on design parameters, but also operational parameters, it is difficult to ensure the stability of such systems in the design phase. There are devices which users can employ to ensure proper pairing of the vehicle and the trailer. Trailer tongue weight scales are often used to check the tongue weight of the trailer and keep it within the limits. After market couplings that allow preloading of friction pads in the ball joints are also available. Although it is known that damping at the joint stabilises the snaking motion (Berntorp, et al., 2014), they are not very effective in increasing the critical velocity of the system ((Darling, et al., 2009) and (Sharp and Fernández, 2002)). Thus, active systems are required to ensure a reasonable improvement.

Different strategies have been explored by researchers to avoid the onset of instability in a vehicle-trailer system. These strategies vary from torque vectoring by differential braking in the wheels to active steering. Strategies based on braking generally utilise two different approaches:

- symmetric braking, to reduce the velocity of the vehicle and let the damping of the vehicle dissipate the oscillations ((Fischer, et al., 2002), (Williams and Mohn, 2004));

- phased braking to generate a stabilising yaw moment (Fernández and Sharp, 2001).

Amongst these, the method of phased braking was found to be more effective (Hac, et al., 2008); however, the use of braking for stabilisation was found to have negative second order effects in the form of an increase in hitch angle which may lead to jacknifing and longitudinal load transfer, resulting in a reduced ability of the rear wheels to apply lateral forces and counter instability. In addition to these, stabilisation through braking invariably results in a reduction in the longitudinal velocity of the vehicle. In their study, Wieven Deng and Xiaodi Kang (Deng and Kang, 2003), developed a control strategy that acted on the steering angle to reduce the hitch angle to an optimum value. The study concluded that:

- feedback with states of both the vehicle and the trailer is necessary;
- the values of hitch angle corresponding to different steady states does not significantly affect the stability characteristics, thus the control design can be independent of the hitch angle value about which the system is linearized.

Mattia Zanchetta and others (Zanchetta, et al., 2018), demonstrated a torque vectoring based control strategy acting on the hitch angle of the vehicle and also concluded, that a control strategy simply acting on the yaw rate of the towing vehicle is not sufficient. However, torque vectoring by means of individual motors was found to be a suitable mode of active stabilisation.

This study presents a simple control strategy based on torque vectoring that does not require any complicated state estimators or expensive sensors to be implemented. Since the motors are capable of applying both driving and braking torque (regenerative braking) they have a considerable range in terms of generating a stabilizing yaw moment. This allows stabilization of the system without a significant reduction in its longitudinal velocity thus increasing its operating range. Further, it avoids the negative second order effects associated with stabilization through braking. In the following, Section 2 reports the equations of the car-trailer system model that were used to simulate the behaviour of both passive and active vehicle. To better understand the nature of the system's instability, Section 3 presents a study of the system eigenvalues and eigenvectors by means of a simplified single-track model. Section 4 presents the proposed active control strategy to stabilize the system; controller equation and preliminary considerations on the controller's effect on system poles is reported. Finally, Section 5 reports the simulation results that were used to validate the controller by comparing the active and the passive vehicles together.

2. MODELLING

The section discusses the non-linear model that has been developed to study the behavior of the system and simulate the performance of the proposed control algorithm.

2.1. Vehicle-Trailer Multibody Model

A 10 degree of freedom model has been developed in the MATLAB Simulink environment to simulate the behaviour of the system and the proposed control strategy. As reported in Figure 1, the following degrees of freedom are considered:

- Longitudinal and Lateral velocity and yaw rate of the vehicle i.e. $\{ v_x \, v_y \, \dot{\psi} \}$
- Yaw rate of the trailer i.e. $\{ \dot{\xi} \}$
- Angular velocities of the wheels i.e. $\{ \omega_{fl} \, \omega_{fr} \, \omega_{rl} \, \omega_{rr} \, \omega_{tl} \, \omega_{tr} \}$

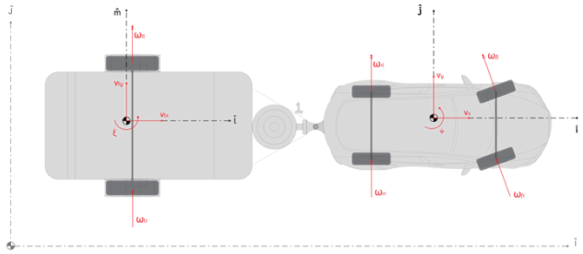

Figure 1. Scheme of the vehicle-trailer model reporting the considered degrees of freedom.

To minimise the complexity of the model, certain assumptions have been made:

- Roll, pitch and heave motions have been neglected
- Suspension system is stiff and road is perfectly smooth
- Load transfer due to longitudinal drag and lift forces are neglected.

Load transfers due to longitudinal and lateral accelerations are accounted by means of 2nd order time lag transfer functions that simulate pitch and roll dynamics.

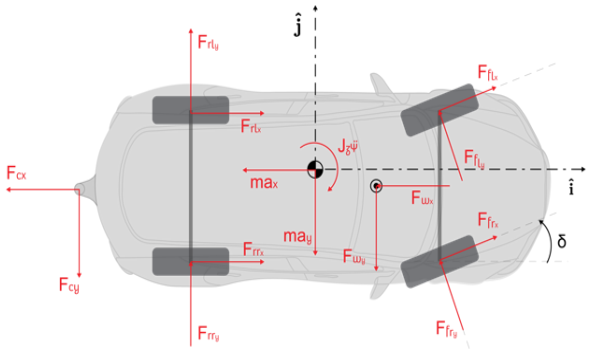

Figure 2. Scheme of forces acting on the towing vehicle

Given those assumptions and making reference to Figure 2, the equilibrium equations for the towing vehicle are;

$$ma_x = \left(F_{fl_x} + F_{fr_z}\right) \cdot cos(\delta) + \left(F_{rl_x} + F_{rr_x}\right) - \left(F_{fl_y} + F_{fr_y}\right) - \left(F_{fl_y} + F_{fr_y}\right) \cdot sin(\delta) - F_{c_x} - F_{w_x} \quad (1)$$

$$ma_y = \left(F_{fl_y} + F_{fr_y}\right) \cdot cos(\delta) + \left(F_{fl_x} + F_{fr_x}\right) \cdot sin(\delta) + \left(F_{rl_y} + F_{rr_y}\right) - F_{c_y} - F_{w_y} \quad (2)$$

$$J_z\ddot{\psi} = \left\{\left(F_{fl_x} + F_{fr_x}\right) \cdot sin(\delta) + \left(F_{fl_y} + F_{fr_y}\right) \cdot cos(\delta)\right\} \cdot a - \left(F_{rl_y} + F_{rr_y}\right) \cdot b + F_{cy} \cdot (b + c) - \left\{F_{fl_x} \cdot cos(\delta) - F_{fl_y} \cdot sin(\delta) + F_{rl_z}\right\} \cdot s_r - F_{w_y} l_{aero} - \left(F_{w_x} + F_{c_x}\right) \cdot \left(s_r - \frac{s}{2}\right) \quad (3)$$

Here, a_x, a_y and $\ddot{\psi}$ represent the longitudinal, lateral and angular acceleration of the centre of gravity of the towing vehicle respectively. δ represents the steering angle at the front wheels. The contact forces are represented by $F_{ij_{x/y}}$ where the indices i and j represent the tyre under consideration. i is f for front and r for rear, while j is l for left and r for right. $F_{c_{x/y}}$refer to the forces at the hitch point while $F_{w_{x/y}}$ refer to the aerodynamics forces due to wind.

The equilibrium equations for the trailer are (see Figure 3);

$$m_t a_{t_x} = F_{tl_x} + F_{tr_x} + F_{ct_x} \quad (4)$$

$$m_t a_{t_y} = F_{tl_y} + F_{tr_y} + F_{ct_y} - F_{tw_y} \quad (5)$$

$$J_{t_z}\ddot{\xi} = F_{ct_y} \cdot d - \left(F_{tl_y} + F_{tr_y}\right) \cdot e - F_{tl_x} s_{l_t} + F_{tr_x} s_{r_t} - F_{tw_y} l_{t_{aero}} + F_{ct_x}\left(s_{r_t} - \frac{s}{2}\right) \quad (6)$$

Here, a_{t_x}, a_{t_y} and $\ddot{\xi}$ represent the longitudinal, lateral and angular acceleration of the centre of gravity of the trailer. The subscript t refers to the trailer.

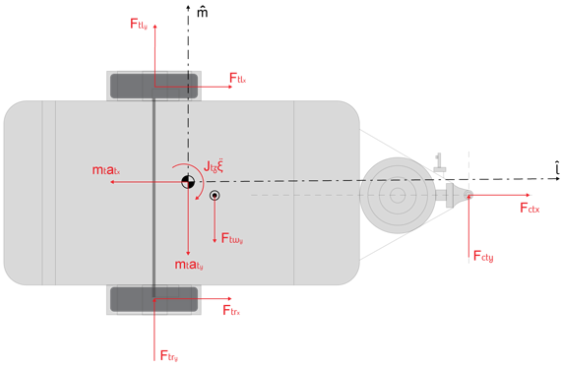

Figure 3. Scheme of forces acting on the trailer.

2.2. Tyre and Wheel Model

The tyre-road contact forces are modelled using the Magic Formula model in the combined form using weighted averages as described in (Berntorp, et al., 2014).

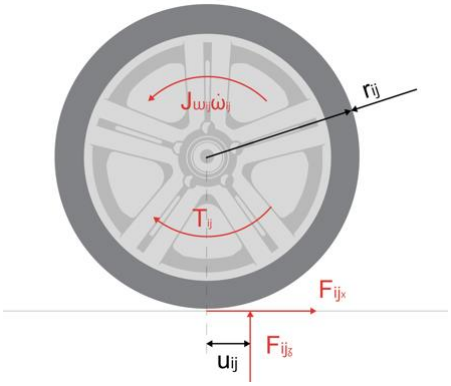

Figure 4. Wheel model

To determine the slip ratio and slip angles, the angular velocity of the corresponding tyre has to be computed, for which the angular velocity of the tyre has to be determined. This is done by performing a moment balance about the centre of the wheel (see Figure 4).

$$\dot{\omega}_{ij} = \frac{T_{ij} - F_{ij_x} r_{ij} - F_{ij_z} u_{ij}}{J_{w_{ij}}} \Rightarrow \omega_{ij} = \int \dot{\omega}_{ij}\, dt + \omega_0 \quad (7)$$

Where, ω_0 refers to the angular velocity of the wheel in steady state condition corresponding to a longitudinal velocity of v_{x0}. The term u_{ij} represents the longitudinal shift of the vertical force to account for rolling resistance and is given as;

$$u_{ij} = f_0 + f_2 v_{x_{ij}}^2 \quad (8)$$

Where f_0 and f_2 are constants depending on the road surface and the tyre. A first order tyre lag model is used to account for the transient behaviour of the tyre in the longitudinal and lateral direction while determining the slip ratios.

$$\dot{\alpha}_{ij} \frac{\lambda_y}{v_{ij_x}} + \alpha_{ij} = -arctan\left(\frac{v_{ij_y}}{v_{ij_x}}\right) \quad (9)$$

$$\dot{\kappa}_{ij} \frac{\lambda_x}{v_{ij_x}} + \kappa_{ij} = \frac{\omega_{ij} r_{ij}}{v_{ij_x}} - 1 \quad (10)$$

To determine the vertical force at each wheel, longitudinal and lateral load transfer has to be determined in which the lateral and longitudinal acceleration and the lateral forces due to wind have been considered. Further, to better simulate real conditions, the lateral load transfer has been distributed between the front and rear axle of the towing vehicle by considering different roll stiffnesses.

2.3. Electric Motors

The electric motors are modelled using their torque speed characteristics. The output of the motors, irrespective of the demand of the controllers, is limited within the maximum/minimum possible torque that the motors can deliver at that particular angular velocity. This is done by means of a dynamic saturation block. Further, a single order time lag transfer function is used to account for the motor dynamics.

2.4. Driver Model

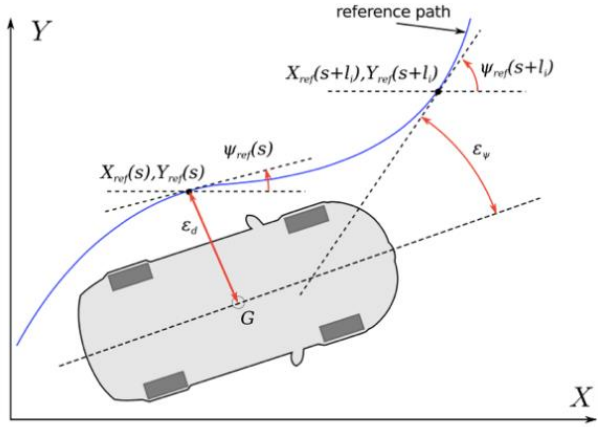

Figure 5. Driver model

A diver model based (see Figure 5) on position and yaw based feedback is used (Sabbioni, et al., 2014). The feedback is based on two preview lengths (l_i) which are a function of the response time of the driver (t_i), and the velocity and acceleration of the vehicle.
For certain manoeuvres, a cruise control logic is used to maintain the longitudinal velocity of the vehicle during the manoeuvre by varying the average longitudinal torque demanded from the motors in the following manner;

$$T_0 = k_{p_{v_x}} \epsilon_{v_x} + k_{i_{v_x}} \int \epsilon_{v_x} dt \quad (11)$$

2.4. Wind Model

A wind model is used to study the effect of gusts on the behaviour of the system. The model generates the velocity of wind as a superposition of two components i.e. average velocity component and a stochastic component which is obtained by filtering white noise through a Dryden filter (Figure **6**). This process allows mimicking the nature of natural gusts. The model has been described in detail in (Hübner, et al., 2008).

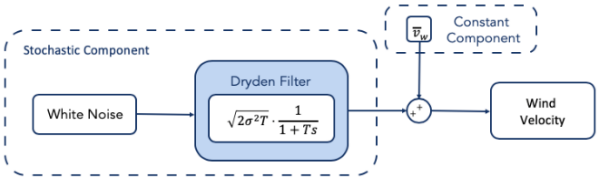

Figure 6. Wind model

Here, σ represents the variance of instantaneous velocity of wind with respect to the average velocity i.e. $\bar{v}_w$ and $1/T$ represents the characteristic wavelength of the natural gusts. The velocity of wind can then be resolved along the local reference systems attached to the centre of gravity of the vehicle and the trailer, to determine the aerodynamic forces acting on the system.

3. STABILITY

The onset of instability is observed beyond certain characteristic velocities, which in turn depend on different parameters. To study the system stability some further simplifications are made. The following section reports the equations of the linearized single-track model used to study the steady-state and dynamic transient behaviour of the system. The first one is analysed by computing the car and trailer understeering gradient while the transient behaviour is studied by computing the linearized system eigenvalues.

3.1. Steady State Behaviour

The steady behaviour of a vehicle is described by means of its understeering coefficient which relates the steering angle required to maintain the path of the vehicle to the Ackerman steering angle. In literature the understeer coefficient of a car without trailer is well known and it is derived starting from the equation for kinematic steering (Wong, 2008)

$$\delta = \frac{l}{R} + \alpha_f - \alpha_r \quad (12)$$

Where δ is the front wheel steering angle, l the car wheelbase, R the radius of the turn and α_f and α_r the slip angles of the front and rear axle respectively. The front axle slip angle α_f can be expressed as a function of the total lateral forces acting at the tyres of the front axle as

$$F_{fy} = \frac{m\,v^2}{R}\,\frac{b}{a+b} = K_f \alpha_f \Rightarrow \alpha_f = \frac{1}{K_f}\,\frac{m\,v^2}{R}\,\frac{b}{a+b} \quad (13)$$

where m is the car mass, v is the vehicle speed, a and b are the semi-wheelbase while K_f is the front cornering stiffness. Similarly, for the rear axle, the rear slip angle is,

$$\alpha_r = \frac{1}{K_r}\,\frac{m\,v^2}{R}\,\frac{a}{a+b} \quad (14)$$

Thus, by substituting values in Eq.$\delta = \frac{l}{R} + \alpha_f - \alpha_r$ (12),

$$\delta = \frac{l}{R}(1 + K_{us}v^2) \quad (15)$$

Where, K_{us} represent the understeering coefficient of the vehicle:

$$K_{us} = \frac{m}{l^2}\left(\frac{b}{K_f} - \frac{a}{K_r}\right) \quad (16)$$

For an understeering vehicle, $K_{us} > 0$. For a neutral vehicle, $K_{us} = 0$, while for an oversteering vehicle $K_{us} < 0$. If the vehicle is oversteering in nature, there exists a threshold velocity beyond which the vehicle becomes unstable. This threshold velocity is obtained by imposing δ as 0 in Eq.$K_{us} = \frac{m}{l^2}\left(\frac{b}{K_f} - \frac{a}{K_r}\right)$ (16) given as;

$$V_{crit} = \sqrt{\frac{1}{-K_{us}}} \quad (17)$$

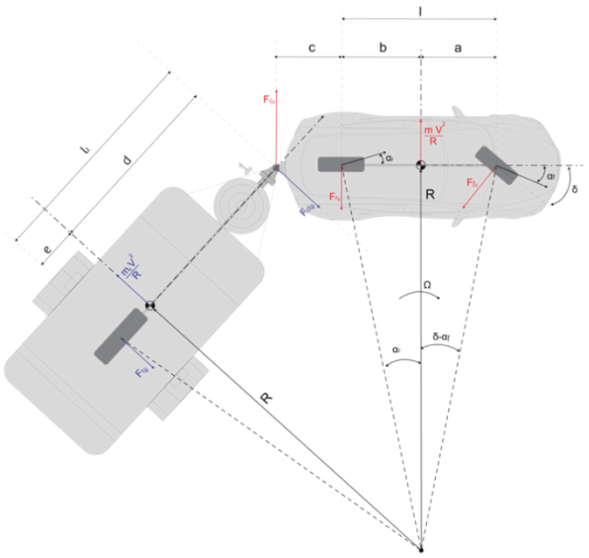

Figure 7. Steady state model.

When a semi-trailer with a single axle is added to the vehicle, it is observed that its understeering coefficient experiences a decrease in its value. Drawing reference to Figure 7;

$$F_{cy} = F_{cty} = \frac{m_t v^2}{R}\frac{e}{d+e} \quad (18)$$

Thus, the lateral forces in the towing vehicle can be evaluated as:

$$F_{fy} = \frac{mv^2}{R}\frac{b}{a+b} - \frac{m_t v^2}{R}\frac{e}{e+d}\frac{c}{a+b} \quad (19)$$

$$F_{ry} = \frac{mv^2}{R}\frac{a}{a+b} + \frac{m_t v^2}{R}\frac{e}{e+d}\frac{a+b+c}{a+b} \quad (20)$$

On substituting the values into Eq.$\delta = \frac{l}{R} + \alpha_f - \alpha_r$ (12), we get:

$$\delta = \frac{l}{R}(1 + (K_{us} - \Delta K)) \quad (21)$$

Where,

$$\Delta K = \frac{m_t}{l^2 l_t}\left(\frac{ec}{K_f} + \frac{e(l+c)}{K_r}\right) \quad (22)$$

The value of ΔK is similar to the value described in (Hac, et al., 2009). Since the value of ΔK is always greated than 0, the value of V_{crit} decreases and directional instability is observed at a lower velocity. The expression of ΔK allows to analyse the effect of different parameters of the system stability. From Eq.$\Delta K = \frac{m_t}{l^2 l_t}\left(\frac{ec}{K_f} + \frac{e(l+c)}{K_r}\right)$ (22), the following consideration can be drawn on the velocity at which directional instability is observed. In particular, the critical speed reduces with:

a. rearward displacement of the centre of mass of the trailer, i.e. decreasing e
b. increasing the wheelbase of the trailer, i.e. l_t
c. decreasing the mass of the trailer, i.e. m_t.
d. increase in the understeering coefficient of the towing vehicle, which in turn, depends on other factors such as; load distribution, torque distribution, roll stiffness, wheelbase of the vehicle etc.

3.2. Dynamic Behaviour

The dynamic transient behaviour of the system is analysed by plotting the poles of the system with increasing velocity.

The model considered for this purpose is a single-track model of the vehicle-trailer system which has four degrees of freedom i.e. $v_x, v_y, \dot{\psi}$ and $\dot{\xi}$ as shown in Figure 8.

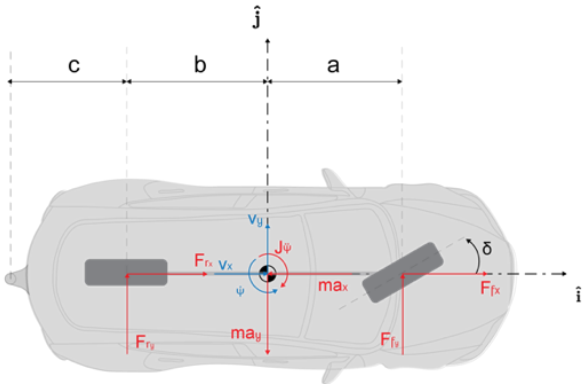

Figure 8. Single track model - car.

By performing force and moment balance for the towing vehicle, we get:

$$ma_y = F_{fy} + F_{ry} - F_{cy} \quad (23)$$

$$ma_x = F_{fx} + F_{rf} - F_{cx} \quad (24)$$

$$J_z\ddot{\psi} = F_{fy}a - F_{ty}b + F_{cy}(b+c) + M_c \quad (25)$$

Here a_x and a_y represent the longitudinal and lateral acceleration of the towing vehicle, while the forces can be seen in Figure 8. Repeating the same for the trailer (see Figure 9):

$$m_t a_{ty} = F_{ty} + F_{cty} \quad (26)$$

$$m_t a_{tx} = F_{tx} + F_{ctx} \quad (27)$$

$$J_t\ddot{\xi} = F_{cty}d - F_{ty}e \quad (28)$$

The subscript t in the above equations represent the trailer. The other indices remain the same as described earlier.

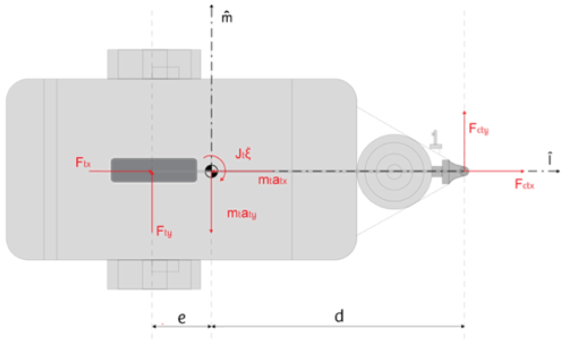

Figure 9. Single-track model – trailer

The contact forces can be determined as a function of slip angles and vertical forces. The slip angle at the front axle is given as:

$$\alpha_f = \delta - arctan\left(\frac{v_y + a\dot{\psi}}{v_x}\right) = \delta - \frac{v_y + a\dot{\psi}}{v_x} \tag{29}$$

Similarly, for the rear axle and the semi-trailer axle:

$$\alpha_r = -\frac{v_y - b\dot{\psi}}{v_x} \tag{30}$$

$$\alpha_t = -\frac{v_y - (b+c)\dot{\psi} - (d+e)\dot{\xi}}{v_x} \tag{31}$$

The contact forces are then given as;

$$\begin{aligned} F_{fy} &= C_f F_{fz} \alpha_f \\ &= C_f \left(mg \frac{b}{a+b} - m_t g \frac{e}{d+e} \frac{c}{a+b} \right) \cdot \left(\delta - \frac{v_y + a\dot{\psi}}{v_x} \right) \\ &= K_f \left(\delta - \frac{v_y + a\dot{\psi}}{v_x} \right) \end{aligned} \tag{32}$$

$$\begin{aligned} F_{ry} &= C_r F_{rz} \alpha_r \\ &= C_r \left(mg \frac{a}{a+b} + m_t g \frac{e}{d+e} \frac{a+b+c}{a+b} \right) \cdot \left(-\frac{v_y - b\dot{\psi}}{v_x} \right) \\ &= K_r \left(-\frac{v_y - b\dot{\psi}}{v_x} \right) \end{aligned} \tag{33}$$

$$\begin{aligned} F_{ty} &= C_t F_{tz} \alpha_t \\ &= C_t \left(m_t g \frac{e}{d+e} \right) \left(-\frac{v_y - (b+c)\dot{\psi} - (d+e)\dot{\xi}}{v_x} \right) \\ &= K_t \left(-\frac{v_y - (b+c)\dot{\psi} - (d+e)\dot{\xi}}{v_x} \right) \end{aligned} \tag{34}$$

By considering the longitudinal speed component v_x to be an input to the system and substituting the values of the contact forces, the equation of motion of the linear single-track model can be given as:

$$\begin{bmatrix} m+m_t & -m_{t(b+c)} & -m_t d & 0 & 0 \\ m(b+c) & J & 0 & 0 & 0 \\ -m_t d & m_t(b+c)d & J_t + m_t d^2 & 0 & 0 \\ 0 & 0 & 0 & 1 & 0 \\ 0 & 0 & 0 & 0 & 1 \end{bmatrix} \begin{bmatrix} \dot{v}_y \\ \ddot{\psi} \\ \ddot{\xi} \\ \dot{\psi} \\ \dot{\xi} \end{bmatrix} =$$

$$\begin{bmatrix} -\frac{K_f + K_r + K_t}{v_x} & -\frac{v_x^2(m+m_t) + K_f a - K_r b - K_t(b+c)}{v_x} & \frac{K_t l_t}{v_x} & -K_t & K_t \\ -\frac{K_f l + K_r c}{v_x} & \frac{-alK_f + K_r cb - m(b+c)v_x^2}{v_x} & 0 & 0 & 0 \\ \frac{K_t l_t}{v_x} & \frac{-K_t l_t(b+c) + m_t v_x^2 d}{v_x} & \frac{-K_t l_t^2}{v_x} & K_t l_t & -K_t l_t \\ 0 & 1 & 0 & 0 & 0 \\ 0 & 0 & 1 & 0 & 0 \end{bmatrix} \begin{bmatrix} v_y \\ \dot{\psi} \\ \dot{\xi} \\ \psi \\ \xi \end{bmatrix} + \begin{bmatrix} K_f & 0 \\ K_f(a+b+c) & 1 \\ 0 & 0 \\ 0 & 0 \\ 0 & 0 \end{bmatrix} \begin{bmatrix} \delta \\ M_c \end{bmatrix} \tag{35}$$

This may be simplified as:

$$[M]\underline{\dot{z}} = [R]\underline{z} + [U]\underline{b} \tag{36}$$

$$\underline{\dot{z}} = [M]^{-1}[R]\underline{z} + [M]^{-1}[U]\underline{b} \tag{37}$$

Where the state vector $\underline{z}$ and the input vector $\underline{b}$ are,

$$\underline{z} = \{v_y \quad \dot{\psi} \quad \dot{\xi} \quad \psi \quad \xi\}^T \tag{38}$$

$$\underline{b} = \{\delta \quad M_c\}^T \tag{39}$$

For a steering input and stabilising moment of $\delta = 0$ and $M_c = 0$ respectively, the poles (eigenvalues) of the system can be plotted as a function of increasing velocity to study the stability of the system. Figure 10 shows that as the velocity of the system increases, the poles move towards the imaginary axis. The poles related to the yaw rate of the vehicle are initially real but become complex conjugate. The poles related to the yaw rate of the trailer are also complex conjugate in nature, and the damping ratio of the system is inversely proportional to the velocity. At a certain velocity, the damping of the system reduces to zero indicated by purely imaginary eigenvalues. A further increase in velocity, results in complex conjugate poles with positive real components, indicating instability.

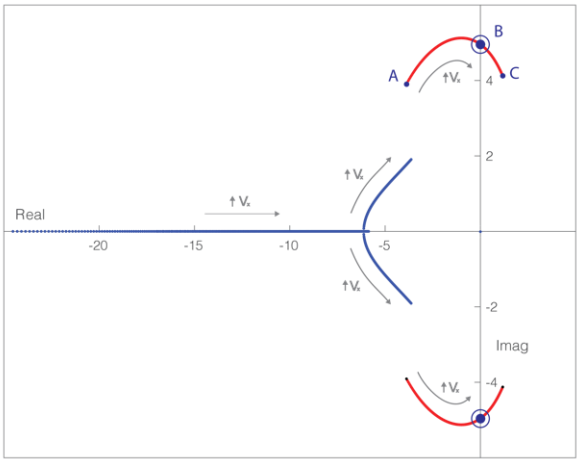

Figure 10. Poles of the system with increasing velocity (e = 0.1 m). The red points represent the poles related to the trailer yaw rate. A - Pole at v_x = 25 km/h; B - Purely imaginary pole a v_x = 83 km/h; C - Pole at v_x = 250 km/h.

Drawing reference to Figure 11, the characteristic velocity at which the damping reduces to zero, decreases from 83 km/h to 76 km/h when the centre of mass of the trailer is moved rearwards by only 0.1 m, while all the other parameters are kept the same. This results in an earlier onset of instability.

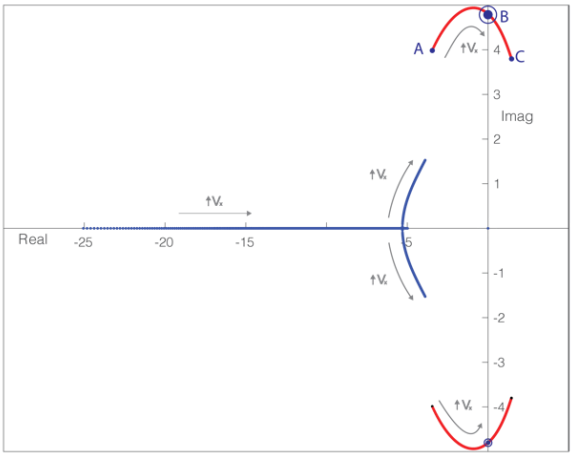

Figure 11. Poles of the system with increasing velocity (e= 0.0 m). The red points represent the poles related to the trailer yaw rate. A-Pole at $\boldsymbol{v_x}$ = 25 km/h; B-Purely imaginary pole at $\boldsymbol{v_x}$ = 76 km/h; C-Pole at $\boldsymbol{v_x}$ = 250 km/h.

There are various other parameters that effect the threshold velocity above which the system becomes unstable. These have been elaborated in various studies ((Hac, et al., 2009), (Hübner, et al., 2008)) and it has been shown that passive systems are not very effective in avoiding instability, although they assist in delaying its onset, albeit by a small degree.

4. CONTROL STRATEGY

Once the stability problems associated to the car-trailer system have been analysed, this section shows the detailed equations of the proposed control strategy that actively damps the trailer oscillations. The proposed control strategy is designed to develop a differential torque (Torque Vectoring) that is superimposed on the average torque requested by the driver or the cruise control system to develop a stabilising yaw moment. The strategy consists of three individual proportional controllers that work in-situ:

- Steady state controller
- Relative yaw rate based controller
- Yaw index based controller

The outputs of the controllers are merged sequentially using linear interpolation based weighted averaging described in (Zanchetta, et al., 2018) allowing the system to behave like a SISO system. The resulting control structure has a hierarchial nature as reported in Figure 12.

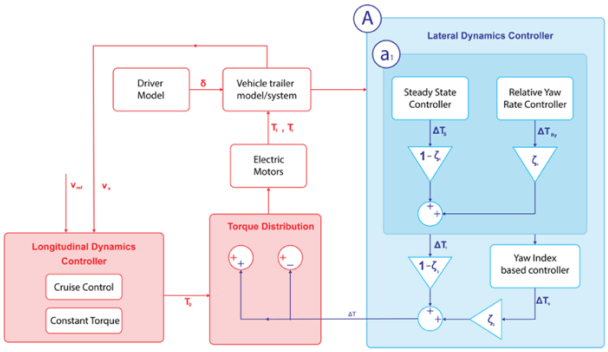

Figure 12. Control strategy

First the hirerchial structure is described following which the three controllers are explained in detail. Drawing reference to Figure 12, the lateral dynamics controller (block A) generates a total yaw moment given by differential torque ΔT which is made of two contributions: ΔT_1 which is the differential torque required to generate the yaw moment necessary to track the yaw rate reference and it is computed in block (a_1); the second contribution is ΔT_{1y} which is the torque difference that generates a yaw moment required to stabilize the car by damping the sideslip angle as better explained in the following.
The output of block (a_1) is ΔT_1 which is the weighted average of the steady state controller (ΔT_s) and relative yaw rate based controller (ΔT_{R_y}) according to the following equation:

$$\Delta T_1 = \zeta_1 \Delta T_{R_y} + (1 - \zeta_1) \cdot \Delta T_S \quad (40)$$

The weight $\zeta_1$varies from 0 to 1 and can be obtained by linearly interpolating the relative yaw rate ($\dot{\tau}$) between a maximum and minimum value and is defined as:

$$\zeta_1 = \begin{cases} 0 & , \ |\dot{\tau}| < \dot{\tau}_{min} \\ \frac{\dot{\tau}_{max} - |\dot{\tau}|}{\dot{\tau}_{max} - \dot{\tau}_{min}} & , \ \dot{\tau}_{min} \leq |\dot{\tau}| < \dot{\tau}_{max} \\ 1 & , \ \dot{\tau} > \dot{\tau}_{max} \end{cases} \quad (41)$$

This contribution is mainly demanded to track the reference yaw rate of the car plus trailer. The resulting torque i.e. ΔT_1, is then merged with the differential torque determined by the yaw index based controller in a similar fashion; however, the weight is dependent on the Yaw Index (I_Y, see Section 3.3) of the towing vehicle (Figure 12(A)). Thus:

$$\Delta T_2 = \zeta_2 \Delta T_{I_y} + (1 - \zeta_2) \cdot \Delta T_1 \quad (42)$$

Where

$$\zeta_2 = \begin{cases} 0 & , \ |I_y| < I_{y_{min}} \\ \frac{I_{y_{max}} - |I_y|}{I_{y_{max}} - I_{y_{min}}} & , \ I_{y_{min}} \leq |I_y| < I_{y_{max}} \\ 1 & , \ I_y > I_{y_{max}} \end{cases} \quad (43)$$

The torque output of the controller is thus given as

$$\Delta T = \xi_2 \Delta T_{I_y} + (1 - \xi_2) \cdot \{\xi_1 \Delta T_{Y_r} + (1 - \xi_1) \cdot \Delta T_s\} \quad (44)$$

This differential torque is then superimposed on the average torque determined by the cruise control logic (refer Eq. $T_0 = k_{p_{v_x}} \epsilon_{v_x} + k_{i_{v_x}} \int \epsilon_{v_x} dt$ (11)) or the demanded constant torque to perform torque vectoring;

$$T_{L,R} = T_0 \pm \Delta T \quad (45)$$

The following three subsections describe the three individual controllers that have been used.

4.1. Steady State Controller

Steady state controller aims at improving the steady state behaviour of the system by acting on the feedback of the yaw rate of the towing vehicle. The controller is a proportional controller where the differential torque expression is:

$$\Delta T_s = \mathrm{K_s} \cdot (\dot{\psi}_{ref} - \dot{\psi}) \quad (46)$$

where $\dot{\psi}_{ref}$ is the reference yaw rate that is obtained by calculating the yaw rate of a kinematical ideal vehicle as a function of the steering input and saturating it to account for the available friction (Vignati, et al., 2016). Making reference to Figure 13, far from friction limit, the yaw rate has a linear relationship with the steering angle according to the following equation

$$\delta = \delta_{ack} \cdot (1 + K_{us} v^2) = \frac{l\dot{\psi}}{v} \cdot (1 + K_{us} v^2) \quad (47)$$

$$\Rightarrow \dot{\psi}_{ideal} = \frac{v}{l \cdot (1 + K_{us} v^2)} \delta = \psi \delta \quad (48)$$

For a neutral vehicle, $K_{us} = 0$. This value can be tuned by the designer of the controller to obtained different vehicle behavior. The yaw rate reference value has to be saturated to account for the available friction i.e. μ.

$$\dot{\psi}_{max} = \frac{\mu g}{R} \quad (49)$$

To smoothen the transition during saturation, an exponential function is used, which allows us to define the reference yaw rate as a function of the steering angle (Figure 13):

$$\dot{\psi}_{ref} = \begin{cases} \dot{\psi}_{ideal} & , \ |\delta| \leq \delta_1 \\ \dot{\psi}_1 + (\dot{\psi}_{max} - \dot{\psi}_1) \cdot \left(e^{-\frac{\dot{\psi}(|\delta| - \delta_1)}{\dot{\psi} - \dot{\psi}_1}} \right), & |\delta| > \delta_1 \end{cases} \quad (50)$$

The effect of this controller on the system is first analysed by computing the poles of the controlled system. Figure 14 reports the root locus of the system for increasing values of K_s.

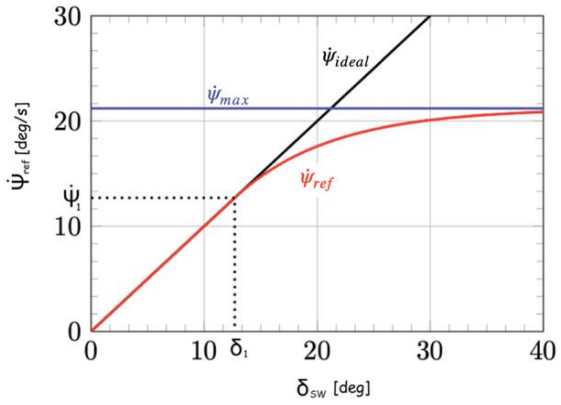

Figure 13. Reference yaw rate

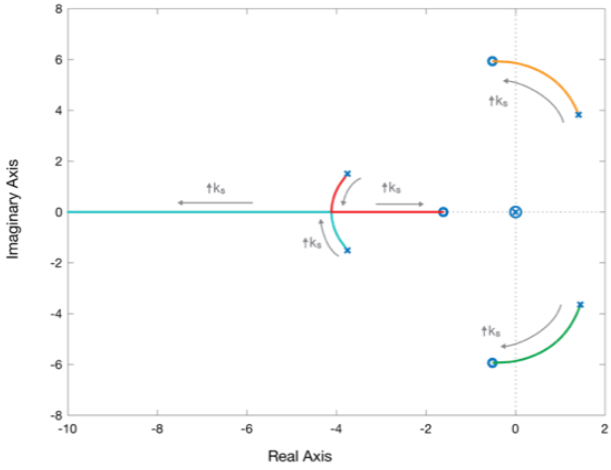

Figure 14. Poles of the system with varying $\boldsymbol{K_s}$

As it can be noticed, considering an unstable passive vehicle (speed higher than critical value which causes the snaking mode to have negative damping), the controller is effective in stabilizing the system for increasing values of K_s. For the system (non-linear model), the value of K_s is obtained by using the Simulink control systems toolbox and the absolute value ($|\Delta T_s|$) of the controller output is limited within a reasonable value by means of a saturation block which accounts for motor torque characteristics.

4.2. Relative Yaw Rate Controller

The aim of this controller is to stabilise the trailer by acting on the relative yaw rate of the towing vehicle and the trailer. This allows the controller to increase the damping of the system related to the trailer yaw rate as can be seen in Figure 15. The controller can be mathematically described as:

$$\Delta T_{Y_r} = K_{Y_r}\left(\dot{\psi} - \dot{\xi}\right) = K_{Y_r}\dot{\tau} \tag{51}$$

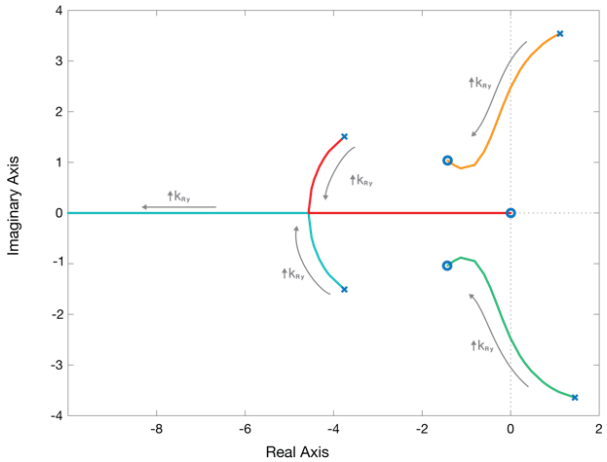

Figure 15. Poles of the system with varying $\boldsymbol{K_{Y_r}}$

4.3. Yaw Index Based Controller

The controller is responsible for improving the transient behaviour of the towing vehicle by opposing to the increase of sideslip angle derivative. It does this by acting on the Yaw Index of the towing vehicle, which represents the rate of change of the side slip angle of the towing vehicle for a constant velocity manoeuvre. The lateral acceleration of the towing vehicle can be described as;

$$a_y = \dot{v}_y + v_x\dot{\psi} \quad (52)$$

Now, $v_y = Vsin\beta$ and $v_x = Vcos\beta$, and for small side slip angles, $sin\beta = 0$ and $cos\beta = 0$. Where, β is the side slip angle. Thus, on substituting the values for a constant velocity manoeuvre;

$$a_y = \frac{d(Vsin\beta)}{dx} + v_x\dot{\psi}$$
$$= \dot{V}sin\beta + Vcos\beta \cdot \dot{\beta} + v_x\dot{\psi}$$
$$= v_x\dot{\beta} + v_x\dot{\psi} \quad (53)$$

$$\dot{\beta} = \frac{a_y}{v_x} - \dot{\psi} = I_y \quad \text{i.e. Yaw Index} \quad (54)$$

The controller can be mathematically described as;

$$\Delta T_{I_y} = K_{I_y} \cdot \left(a_y - v_x\dot{\psi}\right) \quad (55)$$

The effect of the controller on the system can be observed in Figure 16.

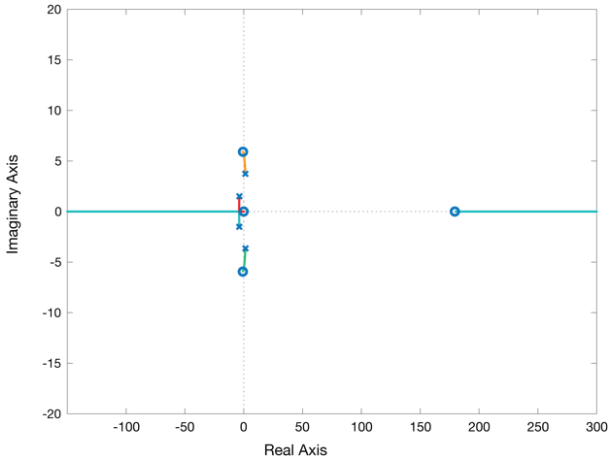

Figure 16. Poles of the system with varying $\boldsymbol{K_{I_y}}$

By means of this strategy (Figure 12), the following is ensured;

a) When the yaw index is high, the weightening coefficient ζ_2 appearing in eq.(42) is high. The resultant torque is largely dependent on the yaw index based controller and focuses on stabilising the vehicle in limit handling conditions.

b) When the yaw index is low, ζ_2 is low. Hence, the contribution of the yaw index based controller is low and the resultant torque is dependent on the steady state controller and the relative yaw rate based controller in the following manner;

- If relative yaw rate is high, ζ_1 is high. The controller output has a high dependence on the relative yaw rate controller and focuses on reducing the relative yaw rate.

- As the relative yaw rate decreases, the value of ζ_1 decreases and the torque output of the controller has a larger dependence on the steady state controller.

Thus, once the vehicle and trailer stabilise, the controller focuses on improving the steady state handling behaviour of the system.

4. SIMULATION RESULTS

The performance of the control strategy has been verified by means of various simulations performed using the non-linear double track model described in Section 2. Only the most significant simulations are reported here.

5.1. Steady State Behaviour

The steady state behaviour of the system was studied by means of a constant radius steering pad manoeuvre with a radius of 100m. The results can be observed in Figure 17 where the steering ratio (steering angle divided by kinematic ackermann steering angle) is reported as a function of vehicle lateral acceleration.

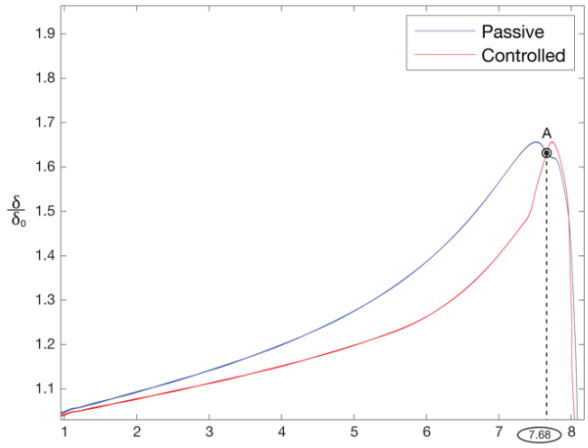

Figure 17. Steering angle ratio Vs. lateral acceleration of car

Figure 18 reports the applied torques on the rear wheels as a function of the car's lateral acceleration. The control strategy improves the steady state behaviour of the system and reduces its tendency to understeer, seen in Figure 17, where the ratio of the steering angle to the ackerman steering angle is significantly lower for the controlled system.
This improvement in the handling behaviour is due to a yaw moment generated through torque vectoring that causes the vehicle to steer inwards (see Figure 18). However, this behaviour is only observed up to a lateral acceleration of 7.68 m/s^2, beyond which the torque in the motors saturate. When this happens, the controller is not capable of further increasing the car lateral acceleration without reducing the δ/δ_0.

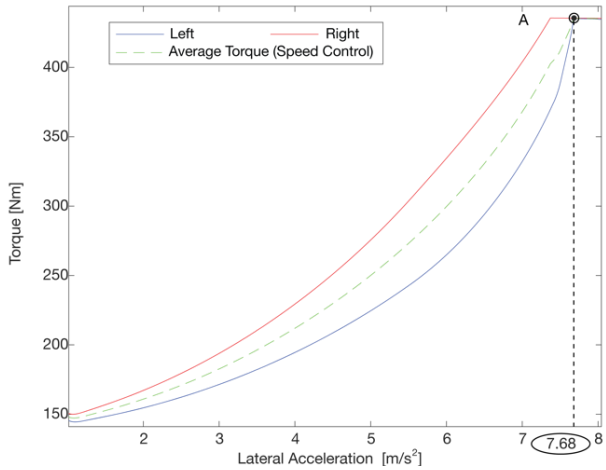

Figure 18. Torque distribution Vs. lateral acceleration of car

5.2. Open Loop Manoeuvre

To analyse the vehicle response in transients without coupling effects with driver, two manoeuvres are simulated: a sine dwell and a step steer.

5.2.1. Sine dwell manoeuvre

A sine dwell manoeuvre consists of a steer and counter steer manoeuvre performed at 0.7 Hz, within the frequency range in which instability is observed. During which, the average torque is determined by the cruise control logic (refer Eq.$T_0 = k_{p_{v_x}} \epsilon_{v_x} + k_{i_{v_x}} \int \epsilon_{v_x} dt$ (11)) to maintain the longitudinal velocity of the vehicle.

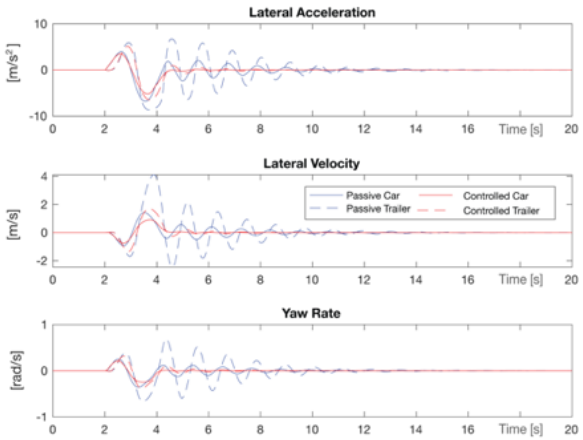

Figure 19. Vehicle response to sine dwell manoeuvre at reference velocity of 85 km/h

At 85 km/h, the passive vehicle demonstrates significant oscillations in the yaw plane with a long settling time while the controlled vehicle immediately stabilises as seen in Figure 19. The control strategy manages to stabilise the system up to a longitudinal velocity of 140 km/h (see Figure 20) while the passive vehicle spins. Further, a very small variation is observed in the longitudinal velocity during the manoeuvre Figure 21.

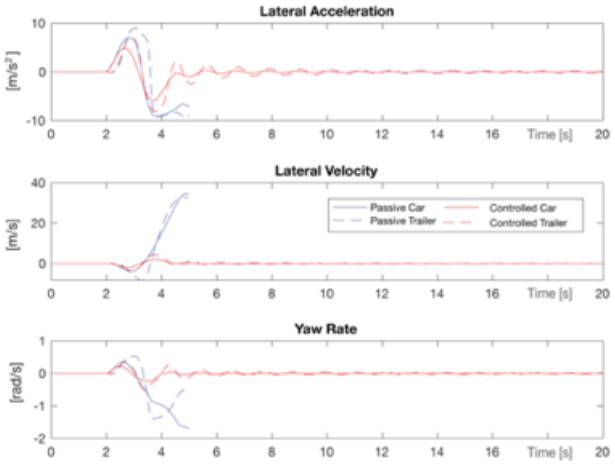

Figure 20. Vehicle response to sine dwell manoeuvre at reference velocity of 140 km/h

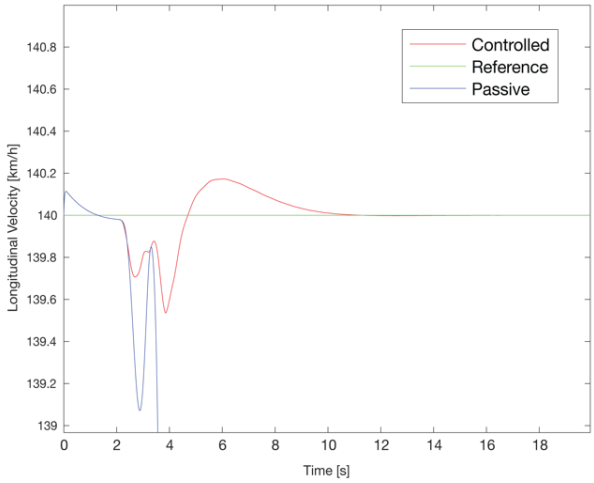

Figure 21. Longitudinal velocity of the vehicle in response to sine dwell manoeuvre at a reference value of 140 km/h

5.2.2. Step steer manoeuvre

The manoeuvre involves introducing a steering input suddenly and maintaining it until the vehicle reaches a steady state. During the manoeuvre, the average torque in the motors was maintained at a constant value as per standards (ISO 7401).

At an entry velocity of 80 km/h, both passive and controlled vehicles are stable (Figure 22); however, the torque distribution in the controlled vehicle reduces its understeering tendency as can be seen in Figure 23; which confirms the results of the constant radius steering pad manoeuvre depicted in Figure 17.

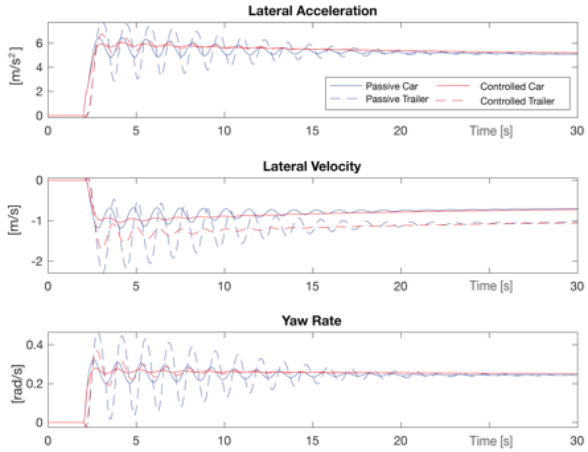

Figure 22. Vehicle response to step steer manoeuvre at entry velocity of 80 km/h

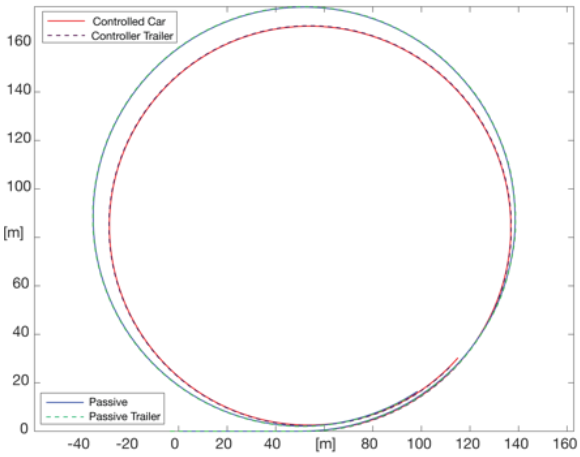

Figure 23. Vehicle trajectory for step steer input at entry velocity of 80 km/h

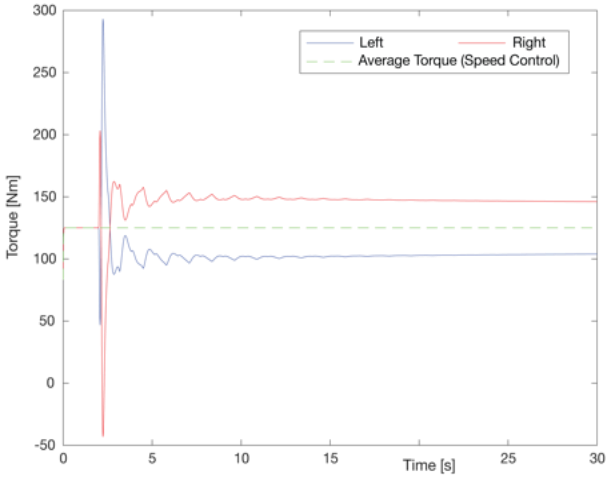

Figure 24. Torque distribution in response to step steer manoeuvre at entry speet of 80 km/h

This reduction in the understeering tendency of the vehicle is a consequence of a higher torque being sent to the outer wheel by the steady state controller (Figure 24), generating a yaw moment that causes the vehicle to steer inwards.
The manoeuvre was also repeated at an entry velocity of 110 km/h in which the passive vehicle spins, while the controlled vehicle manages to complete the manoeuvre (Figure 25). To ensure that the stabilisation is an effect of torque vectoring introduced by the controller and not due to a reduction in velocity, the manoeuvre was repeated with the cruise control system which maintained the longitudinal velocity of the vehicle at 90 km/h. The results of this manoeuvre can be seen in (Figure 26) and they confirm the positive effect of the control strategy.

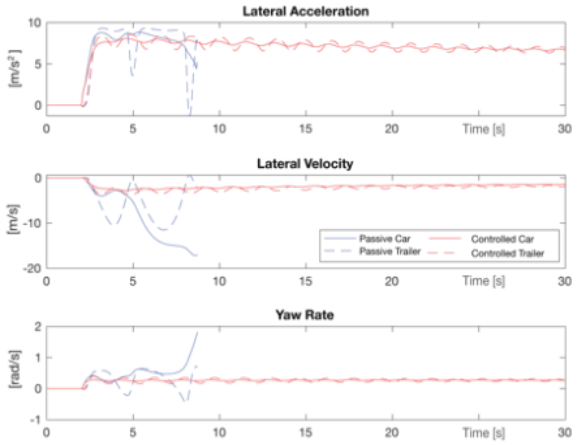

Figure 25. Vehicle response to step steer at entry velocity of 110 km/h

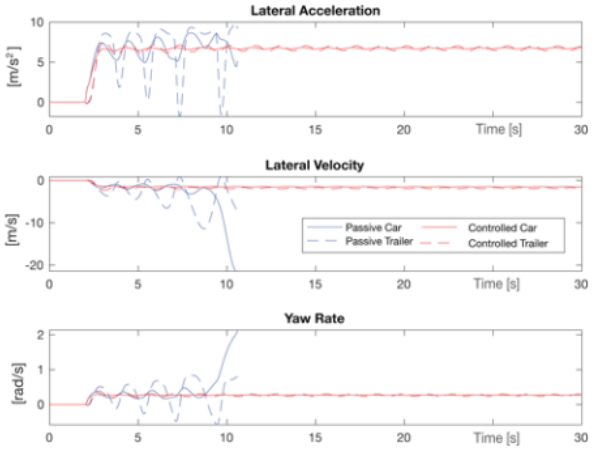

Figure 26. Vehicle response to step steer at 90 km/h (with cruise control)

5.2. Driver in loop manoeuvre

A driver in loop manoeuvre was performed to study the behavior of the system under the effect of lateral gusts. In this manoeuvre the driver is made to follow a straight path at a velocity significantly higher that the critical velocity of the vehicle. The average torque in

the motors is determined by the cruise control system to maintain the average velocity of the vehicle at 140 km/h. At a time, t = 10 s, a lateral gust with an average velocity of 30 m/s is introduced. This time corresponds to the vehicle exiting a tunnel. The instantaneous velocity of the lateral gust is determined by means of the wind model described in Section 2.4. In addition, to ensure compatibility between the simulations, the same time series of the wind velocity was used for both the passive vehicle and the controlled vehicle.

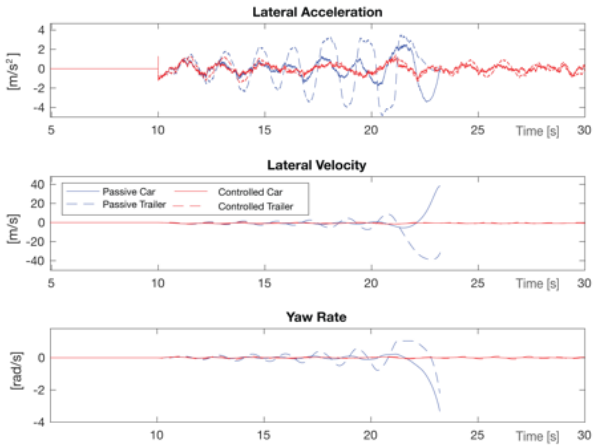

Figure 27. Vehicle respunse to lateral wind gusts of 30 m/s at a longitudinal velocity of 140 km/h

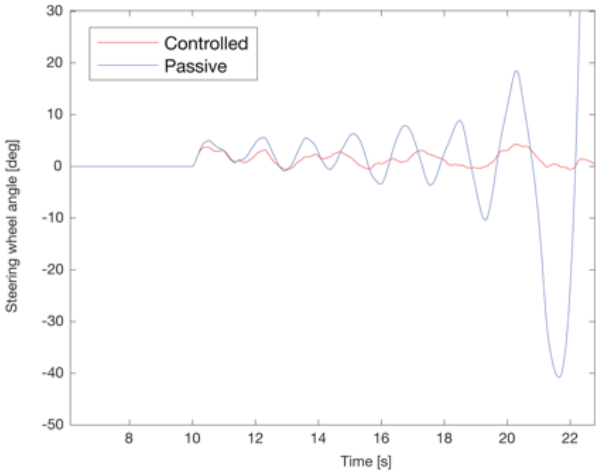

Figure 28. Steering angle imposed by the driver at the steering wheel in response to path deviation due to lateral gust

The passive vehicle, on encountering the lateral gusts at the exit of the tunnel, exhibits increasing oscillations in the yaw plane up to a point where it spins. On the contrary, the controlled vehicle manages to minimise the oscillations in both the vehicle and the trailer as is evident from Figure 27. The oscillations however, persist in the controlled vehicle, as the velocity of the gust keeps on changing.

It is observed that the driver plays a major factor in inducing the instability as can be seen from Figure 28. The lateral gust causes the vehicle to stray from its path, in response to which, the driver introduces a corrective manoeuvre. Since the velocity of the vehicle is

higher than its critical velocity, the corrective manoeuvre induces instability in the vehicle. This is avoided in the controlled vehicle.

6. CONCLUSION

The study clearly shows that the proposed control strategy is able to quickly eliminate the oscillation in the yaw plane in both the trailer and the towing vehicle. Moreover, it is also able to improve the steady state handling behaviour of the system. A clear advantage of this control strategy is there is no dependence on any complicated estimators. The data required for the controllers can easily be acquired by means of cheap sensors.
There are, however, certain limitations in the system which need to be addressed before industrial level implementation. The system in its current architecture, utilises an Inertial Measurement Unit (IMU) in the trailer to determine its yaw rate. This needs a dedicated CAN BUS from the trailer to the towing vehicle, which can be overcome by using sensors in the vehicle to sense the yaw rate of the trailer. In addition, tuning the gain of the controllers, based on the velocity of the system can prove beneficial.

REFERENCES

Berntorp, K., Olofsson, B., Lundahl, K. and Nielsen, L. (2014). Models and methodology for optimal trajectory generation in safety-critical road-vehicle manoeuvres. *Vehicle System Dynamics*, **52**, **10**, pp. 1304-1332.

Bouteldja, M. and Cerezo, V. (2011). Jacknifing Warning for Articulated Vehicles Based on A Detection and Prediction System. *3rd International Conference on Road Safety and Simulation*, Indianapolis.

Darling, J. and Standen, P. M. (2003). A study of caravan unsteady aerodynamics. *Journal of Automobile Engineering*, **217**, **7**, pp. 551-560.

Darling, J., Tilley, D. and Gao, B. (2009). An experimental investigation of car-trailer high-speed stability. *Journal of Automobile Engineering*, **223**, **4**, pp. 471-484.

Deng, W. K. and Kang, X. (2003). Parametric study on vehicle-trailer dynamics for stability control. *SAE Technical Paper 2003-01-1321*.

Fernández, M. A. and Sharp, R. (2001). Caravan active braking system-effective stabilisation of snaking of combination vehicles. *SAE Technical Papers 2001-01-3188.*

Fischer, G., Heyken, R. and Trächtler, A. (2002). Active stabilisation of the car/trailer combination for the BMW X5. *ATZ worldwide* , **104**, pp. 7-10.

Hübner, M., Stork, T., Becker, U. and Schnieder, E. (2008). Lateral stabilization of vehicle-trailer combinations against crosswind disturbances by means of sliding control. *16th Mediterranean Conference on Control and Automation*, Ajaccio, pp. 431-438.

Hac, A., Fulk, D. and Chen, H. (2009). Stability and control considerations of vehicle-trailer combination. *SAE Int. J. Passeng. Cars - Mech. Syst*, **1**, **1**, pp. 925-937.

Sabbioni, E., Cheli, F., Vignati, M. and Melzi, S. (2014). Comparison of Torque Vectoring Control Strategies for a IWM Vehicle. *SAE Int. J. Passeng. Cars - Electronic and Electrical Systems*, **7**, **2**, pp. 565-572.

Sharp, R. and Fernández, M. A. (2002). Car-caravan snaking Part 1: The influence of pintle pin friction. *Proceedings of the Institution of Mechanical Engineers, Part C: Journal of Mechanical Engineering Science*, **216**, **7**, pp. 707-722.

Vignati, M., Sabbioni, E. and Cheli, F. (2016). Torque vectoring control for IWM vehicles. *International Journal of Vehicle Performance*, **2**, **3**, p. 302.

Williams, J. M. and Mohn, F. W. (2004). Trailer stabilization through active braking of the towing vehicle. *SAE Technical Paper 2004-01-1069.*

Zanchetta, M. et al. (2018). On the feedback control of hitch angle through torque-vectoring. *IEEE 15th International Workshop on Advanced Motion Control (AMC)*, Tokyo, pp. 535-540.

Wong, J. Y. (2008). *Theory of Ground Vehicles.* 4 ed. John Wiley and Sons.